THE ASTROPHYSICAL JOURNAL, 555:673–684, 2001 July 10

COSMOLOGICAL EVOLUTION MODELS FOR QSO/ACTIVE GALACTIC NUCLEUS LUMINOSITY FUNCTIONS: EFFECTS OF SPECTRUM-LUMINOSITY CORRELATION AND MASSIVE BLACK HOLE REMNANTS

YUN-YOUNG CHOI,[1,2] JONGMANN YANG,[1,2,3] AND INSU YI[4]

Received 2000 May 31; accepted 2001 March 16

ABSTRACT

We investigate a large number of cosmological evolution models for QSOs and active galactic nuclei (AGNs). We introduce a spectrum-luminosity correlation as a new input parameter and adopt the estimated mass function (MF) of massive black holes in the centers of nearby galactic nuclei as a constraint to distinguish among different QSO/AGN models. We explore three basic types of phenomenological scenarios: (1) models with multiple short-lived ($\sim$ a few 10^6–10^8 yr) populations, (2) models with a single long-lived ($\sim 10^9$ yr) QSO population, and (3) models with recurrent QSO/AGN activities that are driven by long-term variabilities of the disk instability type. In each model, we derive the expected theoretical luminosity function (LF) and the MF of black holes that grow through mass accretion. We assess the plausibility of each model based on whether each model's LF and MF are compatible with the observed data. We find that the best fits to the observed LFs are obtained in the model with multiple short-lived populations and without any significant spectral evolution. This finding suggests that the QSO populations may be composed of many short-lived generations ($\sim$a few 10^8 yr) and that there is no significant spectral evolution within each generation. On the other hand, we also show that there is no satisfactory model that can simultaneously account for the observed LF and the estimated MF. We speculate that some of the present-day black holes found in galactic nuclei may have formed without undergoing the QSO/AGN phase.

Subject headings: black hole physics — galaxies: active — quasars: general

1. INTRODUCTION

It has been well established that the observed comoving space density of optically bright QSOs reaches a peak at a critical redshift $z \sim 2$ (e.g., Peterson 1997; Hartwick & Shade 1990; Weedman 1986). A similar trend is also seen in the X-ray evolution (Miyaji, Hasinger, & Schmidt 2000 and references therein). In both cases, the evolution of the luminosity function (LF) is roughly accounted for by the number-conserving luminosity evolution (e.g., Mathez et al. 1996) in which the luminosities of QSOs first gradually decrease at $z > 2$ from their births near $z > 4$ and rapidly decline at $z < 2$. It has recently been questioned whether the X-ray evolution can be adequately described by the pure luminosity evolution (Hasinger 1998; Miyaji et al. 2000). Although the critical redshift at which the QSO activities show a sudden transition is firmly established, it is unclear what determines such a redshift. There have been numerous attempts and models leading to debates as to what physical processes in QSO/active galactic nuclei (AGNs) engines and/or their surroundings determine the basic characteristics of the cosmological evolution of QSOs/AGNs (e.g., Caditz, Petrosian, & Wandel 1991; Small & Blandford 1992; Fukugita & Turner 1995; Yi 1996; Haehnelt, Natarajan, & Rees 1998; Nulsen & Fabian 2000).

In this work, we intend to explore most of the existing classes of QSO/AGN evolution in their broad categories and to make both qualitative and quantitative comparisons among them. The phenomenological scenarios we explore in this work can be roughly classified as follows: First, we consider a class of models in which a single long-lived ($\geq 10^9$ yr) QSO population evolves throughout the cosmological time after birth at high redshifts $z > 4$ (Mathez 1976; Yi 1996; Peterson 1997 and references therein). Second, we study the models in which many short-lived (a few 10^8 yr) QSO populations form and evolve. In these models, the overall observed evolutionary trend is a result of the collective evolution of many different generations of QSOs/AGNs (Haehnelt et al. 1998). In addition, we also explore a specific physical model in which the QSOs' long-term variabilities caused by accretion disk instabilities contribute considerably to the observed QSO LFs (Siemiginowska & Elvis 1997).

In our previous work (see Choi, Yang, & Yi 1999b, 2000 for details), we have already looked into the first of the models, the pure luminosity evolution model (Mathez 1976; Peterson 1997), with the explicit inclusion of the spectrum-luminosity correlation. In this model, all QSOs are long-lived and they become gradually dimmer with their comoving space number density conserved throughout the evolution, i.e., from their roughly synchronous births to the present epoch. We arrived at a conclusion that the accretion flow transition can be accommodated in the QSO evolution with relatively good fits to the observed luminosity evolution. According to this model, however, the smaller mass black holes with the masses less than $10^8\ M_\odot$ in galactic nuclei (Magorrian et al. 1998) cannot be direct remnants of the past QSO activities as the QSOs' black holes grow much more massive than these black holes (see Wandel 1999). In this model, the QSO remnants have to exist in the nuclei of rare massive galaxies. Then, the often discussed massive dark objects in ordinary galaxies (Magorrian et al. 1998) should have formed and grown without experiencing the QSO phase, which does not appear to be a popular proposition.

[1] Center for High Energy Astrophysics and Isotope Studies, Research Institute for Basic Sciences; ychoi@mm.ewha.ac.kr.
[2] Department of Physics, Ewha University, Seoul 120-750, Korea.
[3] Center for High Energy Physics, Kyungpook National University, Daegu 702-701, Korea.
[4] Korea Institute for Advanced Study, Seoul 130-012, Korea.

The second class of models has been studied recently (e.g., Haehnelt & Rees 1993; Haehnelt et al. 1998) and they are specifically based on the idea that the hierarchical build-up of normal galaxies and the evolution of the AGNs/QSOs are closely connected to each other (see also Haiman & Loeb 1998; Cattaneo, Haehnelt, & Rees 1999; Haiman, Madau, & Loeb 1999). It has been claimed that the density evolution model is supported by the recent observational evidences such as the existence of massive black holes (BHs) with 10^6–10^{10} $M_\odot$ (e.g., Franceschini, Vercellon, & Fabian 1998) and the strong correlation in their masses between the supermassive BH and the spheroidal components of nearby galaxies (e.g., Magorrian et al. 1998; see Wandel 1999).

In a specific model of the third type, we assume that some long-term variabilities of QSO/AGN emission are mainly caused by the accretion disk instability of the dwarf novae type (Frank, King, & Raine 1992) and dominate their recurrent activities (Siemiginowska & Elvis 1997), as is occasionally discussed in connection with the origin of high-luminosity QSO activities.

We consider two fundamentally different assumptions that are motivated by the recent works in the general area of accretion disk physics. These assumptions have direct implications on the luminosity evolution of the QSO/AGN and as a consequence are indirectly testable.

The first one of the two is that the change of accretion flow around a central black hole, which powers the QSO/AGN activities, is mainly driven by the change in mass accretion rate. Such a change then results in the correlated spectral and luminosity evolution of QSO. This assumption is based on the observed behavior of black hole X-ray binaries (BHXBs). Some BHXBs show prominent spectral changes that are strongly correlated with the luminosity changes (e.g., Rutledge et al. 1999; Choi et al. 1999a, 1999b, 2000). Although the details of the models accounting for this behavior vary significantly, it is widely believed that the changes in the mass accretion rate is the underlying cause of this phenomenon. For instance, the ADAF models (Narayan, Mahadevan, & Quatert 1998; Yi 1996 and references therein) have enjoyed a relative success in explaining the hard X-ray–emitting states of BHXBs, while the thin-disk models (Frank et al. 1992) have been widely applied to the soft X-ray–emitting states. In these models, the continuous changes in the spectral state is interpreted as changes in the accretion rate and the accretion disk's physical conditions (e.g., Esin, McClintock, & Narayan 1997 and references therein; Rutledge et al. 1999). We assume that the QSOs' luminosity evolution is accompanied by a strong spectral evolution caused by the accretion flow transition (see Choi et al. 1999a for details). The spectral state is determined by the BH mass and the physical accretion rate. The dominating effect is obviously that the resulting luminosity evolution shows distinct evolutionary behavior in different energy bands. The nearly mass scale-invariant nature of the accretion flow properties further supports this assumption (Narayan & Yi 1995).

The second one is that the QSOs luminosities are interpreted as fixed fractions of the bolometric luminosity and each band's luminosity is simply given as a fixed fraction of the bolometric luminosity regardless of changes in the accretion rate. The latter approach is closer to those of the conventional studies carried out so far (Peterson 1997). Although this assumption is not clearly supported by any physical models of accretion flows, the lack of detailed QSO spectral information in different bands makes it hard to rule out this simple but convenient approach.

In §§ 2 and 3, we summarize the evolution models and describe how we determine model parameters in each model. We derive the resulting analytical LFs of QSO/AGN and mass functions (MFs) of BH remnants. In § 4 we draw our conclusions and discuss their implications on how to interpret the observational data.

2. THE MULTIPLE POPULATION MODEL FOR SHORT-LIVED QSOS

In this type of scenario, the formation and evolution of normal galaxies occur within a hierarchical merging of dark matter halos (Peebles 1993), which is closely connected to the formation and evolution of QSOs experiencing short active phases (Haehnelt & Rees 1993; Kauffmann & Haehnelt 2000; Monaco, Salucci, & Danese 2000). It has been generally assumed that a QSO is born (e.g., Nulsen & Fabian 2000 and references therein) or reactivated (e.g., Small & Blandford 1992) when two galaxies merge and that mergers provide the fuel for the newly formed central massive BH. It remains unclear whether during the short, active emission phase, the QSOs' emission spectra show any rapid spectral evolution while their luminosities rise and fall on timescales much shorter than the cosmological evolution timescale. In other words, one could ask how the assumed spectral evolution, which we mentioned above, affects the QSO LFs in this scenario. In the multiple population models, the cosmologically evolving QSO population is composed of many short-lived generations and undergoes a successive rise and fall of QSO activities. If the luminosity-spectrum correlation is applied to the QSO generations, the evolution of an individual short-lived QSO should exhibit some appreciable changes in the spectral emission state with the decreasing mass accretion rate or luminosity after merge-driven trigger of the QSO activity. One of the most significant constraint on this scenario comes from the observed LFs (e.g., *ROSAT* samples by Miyaji et al. 2000) and the MF derived from the radio LF of E/SO galaxies cores (e.g., Salucci et al. 1999).

We describe the several assumptions and parameters involved in deriving the LFs and constructing an evolution model for QSOs. We first need to specify an individual QSO activity in terms of its spectra and luminosities (see Choi et al. 1999b for details). We assume that each QSO begins its activity with a newly formed black hole of mass M and gas accretion flow with a rate, $\dot{M}$, that shows a general decreas as the QSO evolves. The rate decrease is taken for simplicity to be of the exponential form with the characteristic e-folding timescale $t_{\rm evol}$ (e.g., Haiman & Menou 2000)

$$\dot{M} = \dot{M}_0 \exp\,(-t/t_{\rm evol}) \tag{1}$$

where $t = 0$ is taken to be the QSO trigger time (e.g., Yi 1996). The $t_{\rm evol}$ is taken as a fraction of the cosmic time $t_{\rm age} \sim 10^{10}$ yr for a flat universe (i.e., $q_0 = 0.5$) with no cosmological constant and $H_0 = 50$ km s^{-1} Mpc^{-1} and essentially corresponds to the lifetime of a QSO. The accretion timescale t scales with redshift

$$t \propto (1 + z)^{-1.5}\,, \tag{2}$$

and the accretion rate,

$$\dot{m} = \dot{M}/\dot{M}_{\rm Edd} \propto \dot{M}/M\,, \tag{3}$$

is expressed in units of the mass-dependent Eddington accretion rate.

2.1. *The Spectral Evolution Model for Multiple QSO Populations (SEM)*

As $\dot{m}$ decreases after a merging or some other QSO trigger event, QSOs experience two types of spectral transition, from "very high" state (VHS, slim disk, and $\dot{m} > 1$) to "high" state (HS, thin disk, and $0.01 \leq \dot{m} \leq 1$), and subsequently, from "high" state to "low" state (including the "off" state) (LS/OS, ADAF, and $\dot{m} < 0.01$). These transitions are caused by the physical changes in the accretion flows, and the accompanied luminosity change is strongly correlated with the spectral state change (Yi 1996; Choi et al. 1999a, 1999b, 2000; Narayan et al. 1998). This essentially describes the main ingredients in the assumption of spectral evolution. Based on this simple assumption, we show the expected spectral energy distributions in various spectral states of a QSO with a BH mass of $10^8\ M_\odot$ which include the emission from ADAFs (see Fig. 1*a*). The hard X-ray–emitting ADAF emission has been pointed out as a possible source of the diffuse X-ray background (Yi & Boughn 1998; Fabian & Rees 1995; Di Matteo et al. 1999). Figure 1*b* shows the expected luminosity evolution of a long-lived QSO with the evolution timescale

$$t_{\rm evol} = 0.50 t_{\rm age} \simeq 6.4 \times 10^9\ {\rm yr}\ , \qquad (4)$$

where the initial BH mass is $10^8\ M_\odot$ and the initial $\dot{m} = 1$. The different energy bands show different luminosity evolution trends (Choi et al. 1999b), which suggest that the spectral evolution could be distinguishable from the simple non–spectral evolution case in which the luminosity in each band is simply proportional to the bolometric luminosity (see Fig. 1*b*, *dash-dotted line*). The transition of accretion flows from the thin-disk type (HS) to the ADAF type (LS/OS) occurs at the critical accretion rate $\dot{m}_c = 0.3\alpha^2$, where $\alpha = 0.3$ (Yi 1996; Narayan & Yi 1995), and such a transition makes QSO luminosities decrease/increase rapidly at $z < 1$. In particular, the LFs in the hard X-ray band are affected differently by the spectral change (from HS to LS/OS), which is quite distinct from the way other energy bands behave. The bolometric luminosity evolution is primarily determined by the redshift dependence of the evolutionary timescale defined above. That is, the rapid

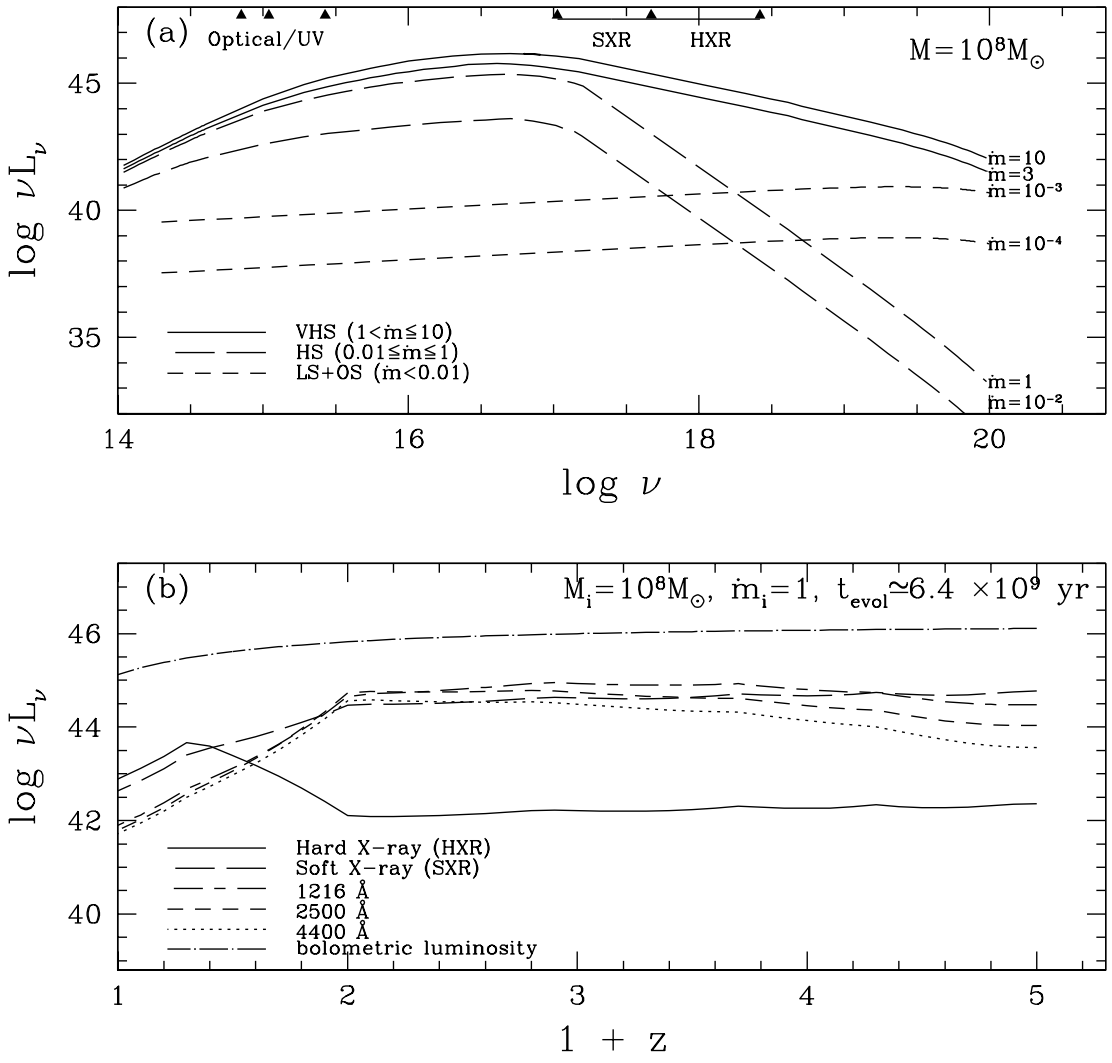

FIG. 1.—(*a*) Spectral energy distributions of a QSO with a BH mass of $10^8\ M_\odot$. From top to bottom, the decreasing $\dot{m}$ causes the spectral and luminosity evolution. VHS, HS, LS+OS denote the very high state, high state, and low state (including the off state), respectively. (*b*) A luminosity evolution of a QSO for $t_{\rm evol} \simeq 6.4 \times 10^9$ yr, with an initial BH mass of $10^8\ M_\odot$, $\dot{m} = 1$. During accretion, different energy bands show different evolutions. At hard X-ray energies, the characteristic transition is identified below $z \sim 1$, at which the luminosity in each band decreases more steeply than the one based on the bolometric luminosity evolution (*dash-dotted line*).

decline of the QSO's bolometric luminosity at low redshifts is caused by the particular redshift dependence of the evolution timescale we have adopted.

We must also specify the several major parameters necessary for the construction of the LF in the SEM model. The main physical parameters are (1) the merger rate of host galaxies or the birth rate of QSOs, (2) the life time of an individual QSO, and (3) the mass distribution of seed BHs at birth. The birth rate in this work is equivalent to the formation rate of new seed BHs at different redshifts. We assume that the birth rate is a simple function of the redshift for which we adopt a simple functional form. For simplicity, we adopt a power law of the form

$$N(z) = N_0[(1 + z)/(1 + z_0)]^s , \quad (5)$$

where N_0 is the number of QSOs belonging to the first generation at the epoch, $z = z_0$, and s determines the basic evolutionary trend of the birth rate as a function of the redshift.

We note that all of the characteristic parameters we find in each evolution model can cause substantial differences to the QSO number density and LF. The best-fit values of the parameters are determined by comparing the resulting LF fits in the soft X-ray band with the observed LFs of AGNs in the same band (e.g., the evolving shape of LFs). Simultaneously, the theoretically predicted mass distributions of remnant BHs are compared with the estimated MF from radio data of E/S0 galaxies (Salucci et al. 1999) and the mass density derived from the massive dark objects (MDOs) mass estimates (e.g., Magorrian et al. 1998). In this sense, the mass distribution of QSO remnants provides an additional constraint (see also Cattaneo, Haehnelt, & Rees, 1999). Such a constraint is of course invalid if a significant fraction of black holes at galactic nuclei are not formed from QSO activities.

Figure 2 clearly shows the dependence of the QSO LF on the three main parameters. In other words, in the SEM models considered, the LFs are essentially determined by the number density in each QSO generation, the number of generations, g, constituting QSOs population, and the evolutionary timescale. QSO LFs shown in this figure refer to those in the soft X-ray energy band, which is identical to the observed soft X-ray band. We assume that the initial accretion rate $\dot{m}$ of an individual QSO dose not exceed the Eddington limit, $\dot{m} = 1$. The comoving number density is normalized to match that of Miyaji et al. (2000) in Figure 2*b*. Figure 2*a*1 gives the best-fit model, which is in good agreement with the observed LFs (see Fig. 2*b*). This particular model assumes with the simple power-law evolution law ($s = -1$) with a broad initial mass distribution of seed BHs, and 100 QSO generations over the range of $0.18 \leq z \leq 4.3$. The $t_{\rm evol}$ for all QSOs is given as $0.03\ t_{\rm age} \simeq 3.9 \times 10^8$ yr. This is in the lifetime range ($\sim 10^6$–10^8 yr) of the luminous phase of QSOs suggested by Haiman & Hui (2000). The initial masses of seed BHs in each generation are randomly chosen by a single power law with a slope of 2.5, and their masses are spread from 10^7 to $10^{10} M_\odot$ in the first high-z generation to 10^6–$10^9\ M_\odot$ in the last low-z generation. Although these assumptions are rather arbitrary, the best-fit model is clearly contrasted with less successful models in fitting the observed LF in Figure 2*b*.

Figure 2*c*1 shows the predicted MF of BHs at six redshifts obtained from LFs (in Fig. 2*a*1), which are in turn derived in the SEM model and Figure *c*2 illustrates that in the single QSO population model (hereafter SES model and see below). The solid line with the cross symbols in Figures 2*c*1 and 2*c*2 represents the estimated MF from radio data of E/SO galaxies in Salucci et al. (1999). According to this model, just a few percent of the present-day galaxies with the comoving number density $\sim 10^{-2}\ h_{50}^3\ {\rm Mpc}^{-3}$ (Magorrian et al. 1998) would have passed through the QSO phase (see Wandel 1999). On the other hand, because of the longevity of the QSOs and the prolonged accretion phase, it is difficult for a single-population model to explain the low-mass BHs with masses of 10^6–$10^7\ M_\odot$ in nearby spiral galaxies (Choi et al. 1999b, 2000 and references therein). In the single-population model, the massive dark objects in the nearby galactic centers cannot have passed through the long QSO phase (see Fig. 2*c*2). It is still possible that some rare massive black holes in giant elliptical galaxies residing in galaxy clusters (Fabian & Canizares 1988; Mahadevan 1997) could have grown through a long-lasting QSO phase. As the number of QSO generations in the SEM model decreases, the resulting LFs become similar to those of the single-population model, as anticipated. The apparent transition from SEM to the single-population model occurs when the number of QSO generations falls to ~ 10 and the QSO evolution timescale $t_{\rm evol} \sim 3.9 \times 10^9$ yr (in Fig. 2*a*4).

One of the distinguishable conclusions concerning this model is that the number density of bright QSOs is not a constant but shows a strong evolution over the cosmological timescale (Miyaji et al. 2000; Wisotzki 2000a). The evolutionary timescale, $t_{\rm evol}$, and its redshift dependence play an important role in causing this feature. In essence, a shorter $t_{\rm evol}$ allows $\dot{M}$ to decline more rapidly and the BHs to gain less mass. For instance, for $t_{\rm evol} = 0.03 t_{\rm age} \simeq 3.9 \times 10^8$ yr, remnant BH masses are bigger than the initial masses by a factor ~ 10. As a result, QSOs experience the sudden changes of the spectral states and a large number of QSOs at any given redshift become too faint to be observed (i.e., less than 10^{42} ergs s^{-1}). This sudden decrease in the number of luminous QSOs gets more marked at lower redshifts owing to the particular redshift dependence of $t_{\rm evol}$. Therefore, unless the power s of the power-law density evolution reverses its sign from positive to negative (from $+1$ to -1), the evolution trend of number density in the derived LF cannot match the observed one. In short, the observed LF evolution requires that the number of QSOs formed at lower redshifts be higher than that at higher redshifts (in Figs. 2*a*1) and 2*a*2). The parameters used in Figure 2*a*2 except for the power s are as given in Figure 2*a*1. Figure 2*a*3 shows that the derived LFs do not evolve significantly if QSOs formed in all generations have the same initial mass distribution in the range of 10^6–$10^9\ M_\odot$. By comparing Figure 2*a*1 with Figure 2*a*3, we see that when the QSOs with less massive seed BHs are born and refueled more abundantly at lower redshifts, the resulting LFs in the SEM model are generally in better agreement with the observed LFs.

Figures 2*a*1, 2*a*4, 2*a*5, and 2*c*1 show the effects of the number of generations and the evolutionary timescale, which directly affect the LF evolution and the MF of the BH remnants. The parameters except for the $t_{\rm evol}$ and the number of generations used in Figures 2*a*4 and 2*a*5 are identical to those given in Figure 2*a*1. If the number of QSO generations is small, the QSO evolution could show some discontinuous evolutionary behavior. In this case, the birth

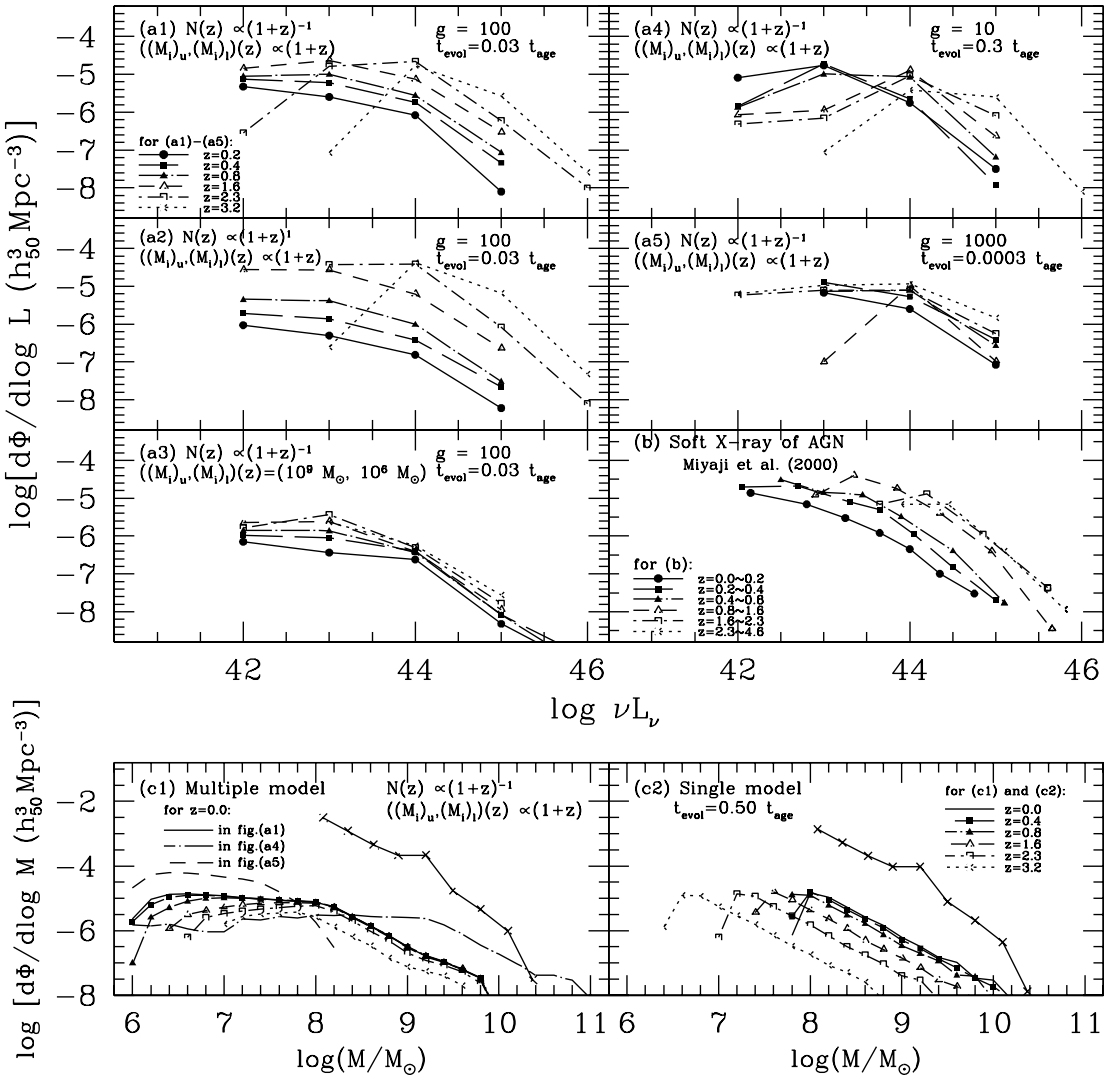

FIG. 2.—(*a*1)–(*a*5) The dependence of the soft X-ray LF of QSOs on several major parameters required in the multiple population model with the spectral evolution correlated with luminosity (i.e., the SEM model): (*a*1) is the best fit in the SEM model; (*a*1) and (*a*2) show the differences due to the functional form of the number density evolution; (*a*1) and (*a*3) show the effects of the initial mass distribution of seed BHs at each generation on LF; (*a*1), (*a*4), and (*a*5) show the effects of superposing multiple generations and varying evolution timescales on LF. (*c*1) The mass distribution of BHs at various redshifts in the multiple population model corresponding to the best-fit model (*a*1). The solid, dash-dotted lines (*without symbols*) and the dashed lines in (*c*1) represent the MF of BH remnants corresponding to the LFs in (*a*1), (*a*4), and (*a*5), respectively, and the solid lines with the cross symbols in (*c*1) and (*c*2) represent the estimated MF from the radio data of E/SO galaxies in Salucci et al. (1999). The comoving number density is normalized to match that of Miyaji et al. (2000); (*c*2) shows the MF in the single-population model.

and death of a generation of QSOs could show up as a discrete evolutionary episode. This type of the discrete evolutionary behavior is smeared out when the number of QSO generations is large enough or the lifetime of QSOs is long enough. For instance, when QSOs in each generation evolve with $t_{\rm evol} \simeq 3.9 \times 10^8$ yr, 100 generations are enough to ensure that the QSO evolution appears smooth and continuous.

2.2. *Constraint from Mass Function of Supermassive Black Hole Remnants*

The MF provides an additional constraint on the QSO evolution. In Figure 2*c*1, the solid, dash-dotted, and dashed lines (*without symbols*) correspond to the predicted MFs of BH remnants in the models with the LFs in Figures 2*a*1, 2*a*4, and 2*a*5, respectively. Because QSOs with a short lifetime do not substantially grow in mass during accretion, in order to match the comoving number density implied by the BH remnant distribution in nearby galaxies, the shorter QSO lifetime demands the higher QSO number density. Figure 2*c*1, however, shows that such a compensation can be ruled out in certain cases, based on the MF. Assuming that the QSOs shine with an X-ray luminosity efficiency of 10% of the bolometric luminosity,

$$L = \eta \dot{M} c^2 \,, \tag{6}$$

with the bolometric radiative efficiency $\eta \simeq 0.1$ during QSO phase, the predicted MF cannot possibly account for the high comoving mass density implied by the nearby galaxies (Salucci et al. 1999).

We find that the comoving number densities of the BH remnants inferred from the best-fitted soft X-ray LF (in Fig. *a*1) are smaller than those estimated for the putative BHs in the bulges of nearby galaxies (e.g., Magorrian et al. 1998; Salucci et al. 1999) by a factor of about 100. This discrepancy has been discussed by several authors (e.g., Small &

Blanford 1992; Phinney 1999; Richstone et al. 1998; Haehnelt et al. 1998). The same number densities we estimate in this model are smaller by a factor of about 10 than those implied by optically bright QSOs under the assumption that they are powered by accretion onto supermassive BHs with an assumed accretion efficiency of 10% (e.g., Phinney 1999; Haehnelt et al. 1998; Richstone et al. 1998 and references therein). These differences are significant, and there do exist some discrepancies between our estimates and the other earlier estimates. Most notably, we use the soft X-ray LF to match the MF of BHs, while other studies adopted the *B*-band LF to match the MF of massive dark objects. In order to allow the predicted MFs to satisfy observational constraint, a number of conditions have to be met. First, the lifetime of sample QSOs must be short (a few 10^6 –10^7 yr) and the QSOs have to be already massive enough (about 10^8–10^{11} $M_\odot$) before accretion-driven mass growth occurs. Such massive black holes could form without emitting detectable photons if their pre-QSO evolution occurs in the form of the super-Eddington accretion with very low radiative efficiencies (Haehnelt et al. 1998). Second, the X-ray fraction of the bolometric luminosity, $f_{\rm XR}$, and/or the bolometric radiative efficiency, η must be smaller than that previously assumed (Haehnelt et al. 1998). For instance, in the absence of any spectral evolution in the context of the multiple QSO population model (hereafter NEM model), the best-fit value of $f_{\rm XR} \times \eta$ is smaller than the usually assumed value by a factor of about 100.

2.3. *No Spectral Evolution Model with Multiple Populations (NEM)*

In Figure 3*a*1 we plot the soft X-ray LF giving the best-fit MF of BH remnants (Fig. 3*c*, *dashed line*) for the model of no spectral evolution of multiple QSO population (hereafter NEM model). In Figures 3*a*2 and 3*c*, the best-fit soft X-ray LF and the MF (*dash-dotted line*) corresponding to this LF are shown. The resulting LF in Figure 3*a*1 is in very poor agreement with the observed LF in Figure 3*b*. Figure 3 demonstrates the difficulty of reconciling the LFs and MFs and fitting them simultaneously.

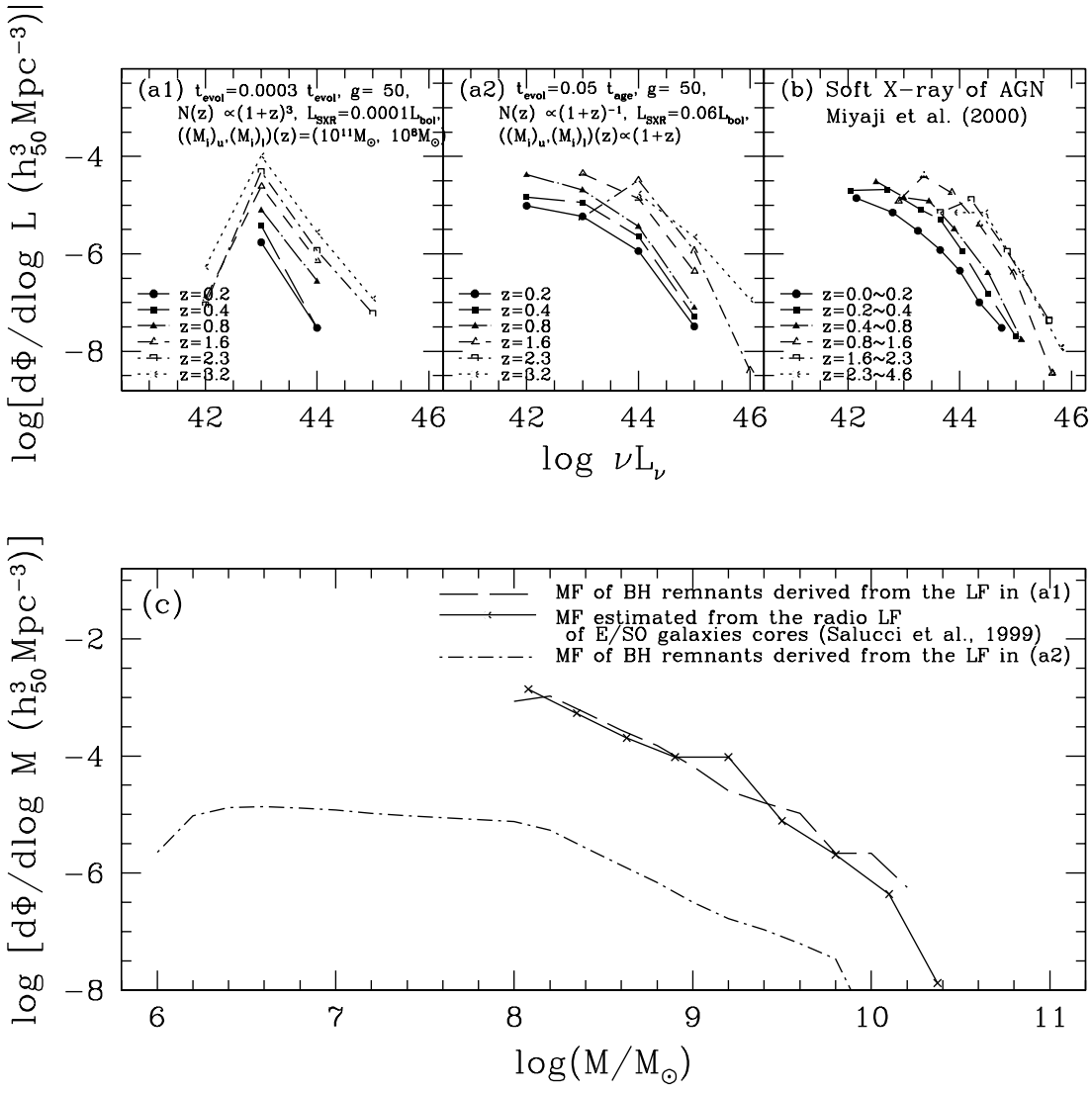

FIG. 3.—Soft X-ray LF in (*a*1) is responsible for the MF of BH remnants (*c*, *dashed lines*) of multiple QSO population without the spectral evolution (i.e., NEM model), which is the best-fit of the MF (*c*, *solid line with cross symbols*) estimated from the radio LF. The parameters required here are given in (*a*1). LF in (*a*2) is the best-fit NEM model for the observed soft X-ray LF of (*b*), and the dash-dotted line in (*c*) represents the MF corresponding to this LF. The comoving number density is normalized to match that of Miyaji et al. (2000) in (*b*).

2.4. *Discrepancies between MF and LF*

There are several possibilities that could potentially account for the discrepancies between the LF and the MF. These possibilities essentially rely on the formation and accretion history for supermassive BHs.

First, the mass density derived from MDOs mass estimates (e.g., Magorrian et al. 1998) could be grossly overestimated owing to some systematic uncertainties in the estimates of $L_{\rm sph}/L_{\rm tot}$, $M_{\rm MDO}/M_{\rm sph}$, etc. (e.g., Salucci et al. 1999). Second, it might be unreasonable for all galaxies to contain MDOs that are actually supermassive BHs. In other words, just a few percent of the present-day galaxies with the comoving number density $\sim 10^{-2}\ h_{50}^3\ {\rm Mpc}^{-3}$ (Magorrian et al. 1998) could have passed through the QSO phase powered by accretion on to supermassive BHs. Third, the low optical emission efficiency could be responsible for low number densities observed in the LFs (Haehnelt et al. 1998). Haehnelt et al. (1998) speculated on two possibilities based on the possibility of the low optical emission efficiency. One of them is the existence of a population of obscured QSO by dust based on the unified Seyfert scheme (e.g., Madau, Chisellini, & Fabian 1994; Comastri, Setti, & Zamorani 1995; Hasinger 2000; Fabian 1999), and the other is the existence of a population of galaxies undergoing ADAF-type accretion (Narayan & Yi 1995; Fabian & Rees 1995; Yi 1996). We emphasize that although we do not use the *B*-band LF but the soft X-ray LF to match the observed soft X-ray LF, our treatment of accretion and QSO emission does include the evolution through the ADAF phase (via spectral evolution). Despite this improvement, which addresses the low-efficiency ADAF flows, the resulting comoving number density of BH remnants is still far short of the required mass density of BHs in nearby galaxies.

The gas and dust obscuration could affect the observed QSO luminosities not only in the optical band but also in the soft X-ray band (Hasinger 2000; Fabian 1999). The effects of obscuration in QSO number counting could be significant and its indirect evidence could be found in the fact that the space density of obscured AGNs is about 3 times higher than that of unobscured AGNs in the X-ray background model (Comastri et al. 1995; Hasinger 1998). The effects of obscuration on emission could differ significantly from band to band. The space density obtained for the soft X-ray of AGNs by Miyaji et al. (2000) exceeds the one observed by Boyle et al. (1991, 2000), which suggests that the optical and X-ray LFs evolve quite distinctly (see Hatziminaoglou, Waerbeke, & Mathez 1998; Wisotzki 2000b). Therefore, we can plausibly conclude that the effects of the low-efficiency accretion as discussed by Haehnelt et al. (1998) are at most marginally significant whereas the possibility of obscured accretion and emission appear to be more important in reconciling the QSO LFs and MFs.

On the other hand, because of the long accretion phase and huge mass gains of QSOs, it is difficult for a single-population model to account for the smaller mass BHs with masses of 10^6–$10^7\ M_\odot$ in nearby spiral galaxies in terms of the QSO remnants that have evolved through the QSO phase (see Fig. 2*c*2). It is also difficult to rule out the possibility that only the more massive black hole remnants have gone through the QSO phase and these giant QSO remnants are found in present-day giant elliptical galaxies. LF in the SEM model with the generations of 10 and $t_{\rm evol}$ of 3.9×10^9 yr (in Fig. 2*a*4) is already nearly indistinguishable from one in the single-population model with spectral evolution.

2.5. *Comparison among Various Evolution Models*

Figure 4 makes a comparison among the derived LFs in various energy bands including hard X-ray energies (2–10 keV), soft X-ray energies (0.5–2 keV), and 4400 Å for all the QSO evolution models we test. The best-fit evolution parameters in each model are determined by requiring them to make the derived the soft X-ray LF in good agreement with the observed LFs of AGNs in the soft X-ray band (Miyaji et al. 2000). Such a fitting also fixes the overall normalization of the comoving number density. The best-fit values of the parameters for various models are shown in the Table 1.

The MFs of BH remnants in Figure 5 result from these best-fitted LFs shown in Figure 4. Figures 4 and 5 clearly demonstrate the difficulties in satisfying the LF and MF constraints simultaneously. In Figures 4*a*1 and 4*b*1 show the derived LFs in various energy bands for SES and SEM models, respectively. It appears that the SEM model gives the LFs in the soft X-ray energy band which are in better agreement with the observed number densities and luminosities evolution of QSOs than the SES model. Such an assessment critically relies on the fact that at $z = 0.8$–1.6 the number densities of the observed bright QSOs (Miyaji et al. 2000) apparently decrease only very gradually. The AGN LFs in the soft X-ray band have been updated by more extensive analyses with more recent and expanded *ROSAT* Bright Survey and *ROSAT* Deep Survey (Miyaji et al. 2000). Together with the earlier results reported by Hasinger (1998), these LFs show an apparent excess at the faintest soft X-ray luminosities less than 10^{42} erg s^{-1} at the redshift epoch of $z = 0.0$–0.2. In this work, we do not consider this excess in deriving the best fits, based on the fact that at such a low luminosity level the distinction between

TABLE 1

BEST-FIT PARAMETERS FOR LFs IN VARIOUS MODELS CONSIDERED

Model[a]	Parameters[b]
SES	$t_{\rm evol} = 0.50 t_{\rm age}$, $z_i = 4(\sigma_z = 0.5)$, $\dot{m}_i = 1(\sigma_{\dot{m}} = 0.1)$
NES	$t_{\rm evol} = 0.25 t_{\rm age}$, $z_i = 4(\sigma_z = 0.5)$, $\dot{m}_i = 1(\sigma_{\dot{m}} = 0.1)$
DSES	$t_{\rm evol} = 0.40 t_{\rm age}$, $z_i = 4(\sigma_z = 0.5)$, $\dot{m}_i = 1(\sigma_{\dot{m}} = 0.1)$; $\Delta \log \dot{m} = 1$, $t_{\rm act}/t_q = 0.25, 10^3$ bursts
DNES	$t_{\rm evol} = 0.25 t_{\rm age}$, $z_i = 4(\sigma_z = 0.5)$, $\dot{m}_i = 1(\sigma_{\dot{m}} = 0.1)$; $\Delta \log \dot{m} = 1$, $t_{\rm act}/t_q = 0.25, 10^3$ bursts
SEM	$t_{\rm evol} = 0.03 t_{\rm age}$, $\dot{m}_i(z) = 1(\sigma_{\dot{m}} = 0.01)$; $g = 50$, $(z_o)_i = 4.3$, $(z_f)_i = 0.18(\sigma_z = 0.001)$
NEM	$t_{\rm evol} = 0.05 t_{\rm age}$, $\dot{m}_i(z) = 1(\sigma_{\dot{m}} = 0.01)$; $g = 50$, $(z_o)_i = 4.3$, $(z_f)_i = 0.18(\sigma_z = 0.001)$
DSEM	$t_{\rm evol} = 0.03 t_{\rm age}$, $\dot{m}_i(z) = 1(\sigma_{\dot{m}} = 0.01)$; $g = 50$, $(z_o)_i = 4.5$, $(z_f)_i = 0.18(\sigma_z = 0.001)$; $\Delta \log \dot{m} = 4$, $t_{\rm act}/t_q = 0.25, 10^3$ bursts
DNEM	$t_{\rm evol} = 0.03 t_{\rm age}$, $\dot{m}_i(z) = 1(\sigma_{\dot{m}} = 0.01)$; $g = 50$, $(z_o)_i = 4.5$, $(z_f)_i = 0.18(\sigma_z = 0.001)$; $\Delta \log \dot{m} = 1$, $t_{\rm act}/t_q = 0.25, 10^3$ bursts

[a] D-: disk instability, SE-: spectral evolution, NE-: no spectral evolution, S-: single QSO population, M-: multiple QSO populations.

[b] $H_o = 50\ {\rm km\ s^{-1}\ Mpc^{-1}}$, $q_o = 0.5$, $\Omega_\Lambda = 0$, $L_{\rm bol}$: bolometric luminosity, $L_{\rm HXR+SXR} = 0.1 L_{\rm bol}$ in SE- series models, $L_{\rm HXR} = 0.04 L_{\rm bol}$, $L_{\rm SXR} = 0.06 L_{\rm bol}$, and $L_{4400\ \text{Å}} = 0.43 L_{\rm bol}$ in NE- series models. The functional forms in the multiple population models correspond to $N(z) = N_o[(1+z)/(1+z_o)]^{-1}$, where N_0 is the number of QOSs belonging to the first generation at the epoch, $z = z_o$. z_f represents the epoch at which the final generation is born.

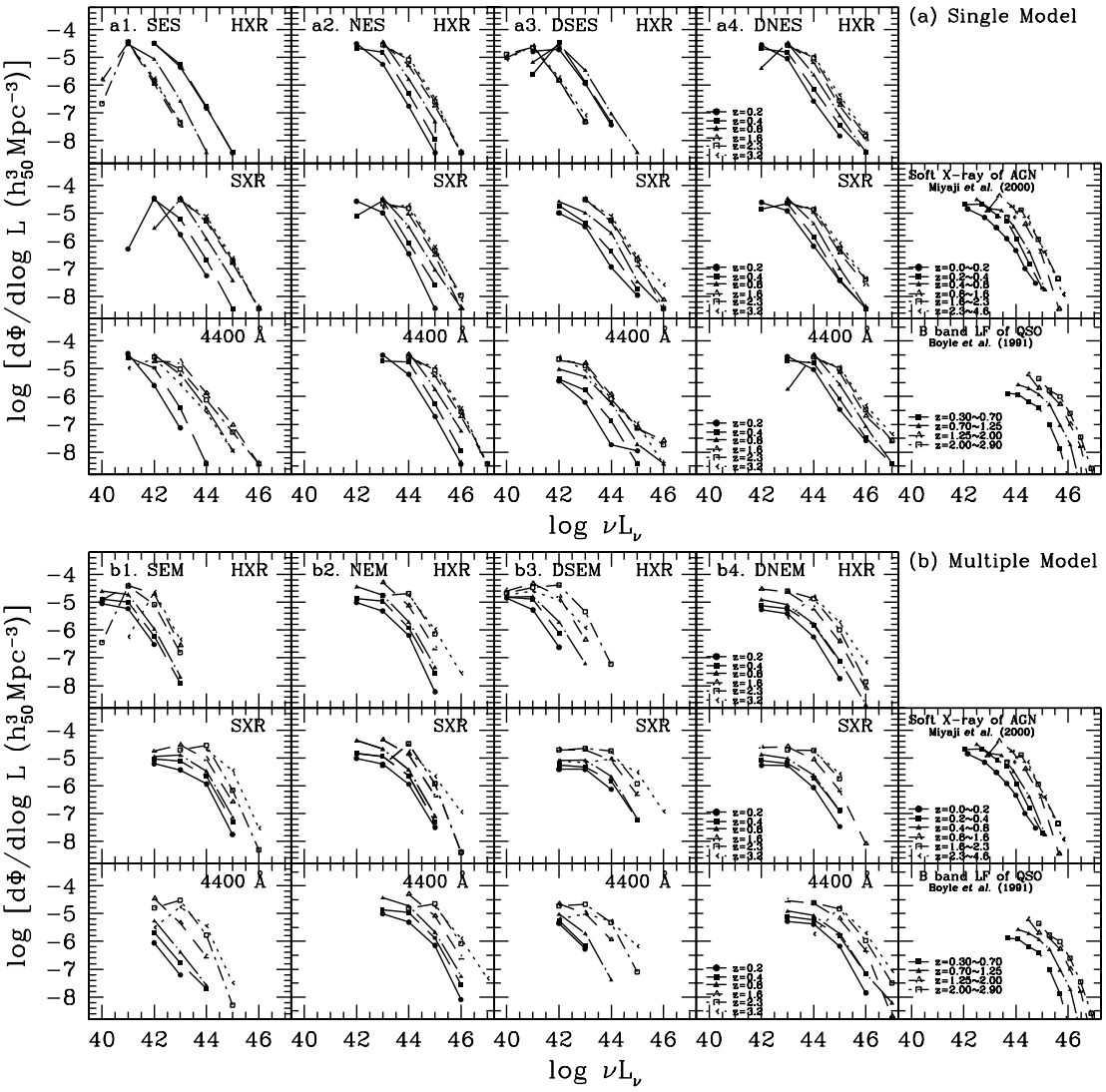

FIG. 4.—Redshift evolutions of the LF for single (S-) and multiple (M-) population models (*a* and *b*, respectively). The LF evolution has been obtained under the set of four assumptions on the luminosity evolution of a QSO; spectral evolution (SE-), no spectral evolution (NE-), and disk instability induced evolutions in both types of spectral evolution (D-). By demanding that we obtain the soft X-ray LF in a good agreement with the observed soft X-ray LFs (Miyaji et al. 2000), we fix the parameters and normalize the comoving number density. The best-fit parameters used in various models are shown in the Table 1.

QSOs/AGNs and less active bright galaxies and/or Seyferts is quite obscure (e.g., Yi & Boughn 1998, 1999 and references therein). For these low-luminosity AGNs, the observed low-energy X-ray background (XRB) could provide an integral constraint on their LFs (e.g., Franceschini et al. 1999).

It is generally difficult to interpret specific best-fit values of the QSO evolution parameters in the multiple population model although in the hierarchical galaxy formation scenario the QSO evolution occurs as a part of the general galaxy formation. In particular, the duration of each QSO generation and the number of QSO generations over the cosmological age of the universe are not well constrained.

We find that just as in the SES model, the SEM model also gives different LF evolution trends in different energy bands. The adopted spectral evolution prescription (Choi et al. 1999b and references therein) causes the optical (4400 Å) LF to evolve much faster than the X-ray LF at lower redshifts. The QSOs in this model are optically much less bright than those in the SES model as well as the observed one (Boyle et al. 1999). In the SES model, the distinctive evolutionary feature at the hard X-ray energies shows up; this feature is essentially summarized as the reversal in the direction of luminosity function evolution and such an apparently puzzling feature is solely due to the accretion flow transition from a thin disk to an ADAF. In the SEM model, however, this effect is cancelled out owing to a successive evolution of multiple generations, a result that does not sensitively depend on the exact number of QSO generations as long as the SEM model has a large enough generations to be qualified as a multiple population model. It is interesting to point out that we can infer from the existence or nonexistence of this particular feature whether the QSO population is composed of multiple generations or a single generation.

2.6. *Multiband QSO Luminosity Evolution*

We now look into how the multiple population model is distinguished from the single-population model if the QSO luminosity evolution is not accompanied by the spectral

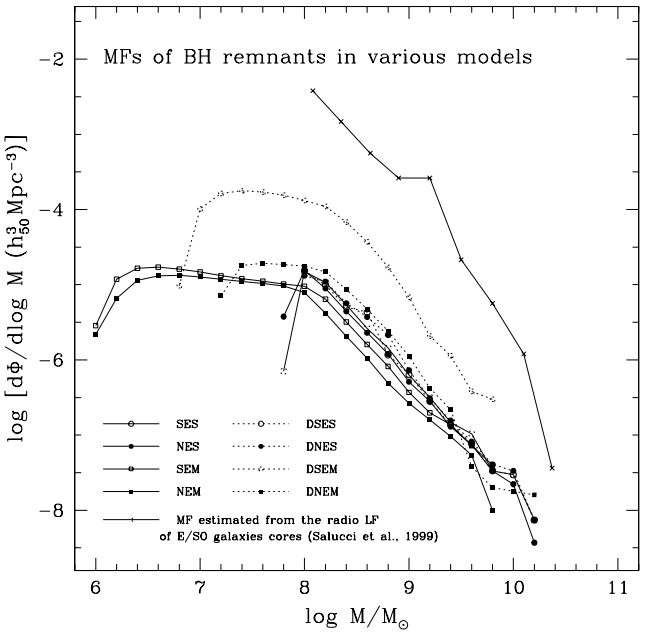

FIG. 5.—MFs of BH remnants corresponding to the best-fitted LFs shown in Fig. 3. The comoving number densities of derived QSO remnants are short of the required numbers for the MF estimated from the radio LF (Salucci et al. 1999).

evolution. In the case of no spectral evolution, the luminosity, L, in each band is simply proportional to the bolometric luminosity, $L_{\rm bol}$, i.e.,

$$L = fL_{\rm bol} = f(\eta \dot{M} c^2)\,, \tag{7}$$

where $\eta \sim 0.1$ is the radiative efficiency. We adopt the fraction f of each band as 0.43, 0.47, 0.06, and 0.04 in the bands 4400 Å,1216 Å, soft X-ray, and hard X-ray, respectively. These fractions have been chosen solely based on the need to fit the observed LF evolution in each band and hence at this point, we do not have any compelling physical motivation for these numbers. As anticipated, the evolution in all bands essentially have similar trends. The fraction of the bolometric luminosity radiated in the optical band of 4400 Å, $f_{4400\text{Å}}$, is about four times larger than the conventionally assumed value, $f_{\rm B} = 0.1$ (e.g., Haehnelt et al. 1998) in our case. We have not considered detailed corrections for dust absorption.

In the absence of the strong spectral evolution induced by the accretion flow transition to low-efficiency ADAFs, the luminosity evolution is generally much slower than in the case of the spectral evolution. An accelerated evolution occurs in which luminosities drop dramatically below the critical mass accretion rate, $\dot{m}_c$. ADAFs appear with their characteristic hard spectra, as shown in Figure 1*b*. In the single-population models with no spectral evolution, the obtained best-fit QSO evolutionary timescale is shorter than that of the spectral evolution case. Figures 4*a*2 and 4*b*2 show the best-fit LFs in various energy bands in the single population no spectral evolution model (hereafter NES model) and no spectral evolution with multiple populations (NEM model), respectively. All parameters used in the case of non-spectral evolution are given in Table 1. The resulting MF of BH remnants in each model is shown in Figure 5. Comparing the SEM model with the NEM model, we find that the NEM model gives the evolving shape of LFs, which fits the observed optical (*B*-band LF of QSO observed by Boyle et al. 1991) *as well as soft X-ray LFs* even if there are no substantial differences in the evolving energy-dependent profiles of LFs in this NE- series models, differently from the observed one. Wisotzki (2000b) attempts to reconcile the discrepant evolution rates of optical and X-ray LFs by modifying an optical LF (i.e., a new determination of the optical K-correction for QSOs). Despite the physical motivation for the spectral evolution, we conclude the NEM model is more plausible in accounting for the observed LF. This result partially supports the possibility that the QSO population is composed of the multiple short-lived (a few 10^8 yr) generations of which the lifetime is short enough to have no significant spectral evolution over each generation's evolution. This is in agreement with the observational result that the spectra in the X-ray bands show no conspicuous variation in the spectral index with redshift (e.g., Blair et al. 2000).

However, it still remains problematic in the NEM model that the BH number density corresponding to the observed soft X-ray LF (Miyaji et al. 2000) is too high to match the number density observed by Boyle et al. (1991). It appears that our results indicate that the optical and X-ray LFs evolve separately with different number densities. For instance, Haiman & Menou (2000) suggest the possibility that the ratio of optical to X-ray emission of quasars could evolve with redshift owing to the cosmological structure formation and accompanying evolution of the QSO environment. The two models, one with the spectral evolution (SEM model) and the other without (NEM model), have substantial differences in the hard X-ray luminosity evolution. Consequently, as previously predicted (Choi et al. 1999b), the observational LF data in the hard X-ray that will be obtained by *Chandra* X-ray observatory could play a role in determining the importance of the spectral evolution.

3. QSO LFS IN THE DISK INSTABILITY MODEL

The observational and theoretical similarities between Galactic X-ray binaries and AGNs in emission mechanisms and spectral behavior lead us not only to assume the QSO spectrum-luminosity correlation but also to expect the QSO accretion flows' time-dependent phenomena similar to those of the Galactic binary systems. Most notably, the occasional outbursts from black hole binaries in the Galaxy could be relevant for AGN/QSO emission from scaled-up accretion flows around supermassive black holes. The enormous differences between Galactic black hole systems and AGNs/QSOs should be reflected in timescales of similar phenomena such as the recurrent outbursts. If the variability due to the thermal-viscous ionization instabilities in accretion disks in cataclysmic variables or X-ray transients does operate in accretion disk in AGNs on longer timescales (Siemiginowska, Czerny, & Kostyunin 1996 and reference therein; Mineshige & Shields 1990), the observed QSO/AGN LFs could be affected by the recurrent outbursts. Siemiginowska & Elvis (1997) assumed that all QSOs are subject to this variability and calculated the LF of a population of identical sources with a single mass and an accretion rate while the possible ADAF-like emission at the low-luminosity end of the light curve was ignored.

Here we consider the disk instability model for QSOs in which QSOs' disk emission is periodically modulated with recurrent outbursts separated by quiescence. We apply our simple assumptions on the luminosity evolution of QSOs to

this disk instability model and derive the LFs and MFs for four sets of evolution models of QSOs: (1) disk instability induced spectral evolution model of a single QSO population (DSES model), (2) disk instability induced nonspectral evolution model of a single QSO population (DNES model), (3) disk instability induced spectral evolution model of multiple QSO populations (DSEM model), and (4) disk instability induced nonspectral evolution model of multiple QSO populations (DNEM model). The resulting LFs and MFs for these disk instability models are included in Figures 4 and 5. In order to obtain the soft X-ray LF in good agreement with the observed LFs of AGNs in the soft X-ray band (Miyaji et al. 2000), the parameters are optimized and the comoving number density is normalized. The best-fit parameters determined for various models are listed in Table 1.

We assume that a single QSO undergoes repeated bright and faint phases. These bright and faint phases correspond to outbursts and quiescent states, respectively. When the spectral evolution model is adopted, the behavior of the low-luminosity part is essentially determined by the ADAF emission. A number of new parameters are introduced in the disk instability models. The major model parameters include the amplitude of accretion rate variation, duty cycle between the active phase and the quiescent phase, and the number of bursts. We assume that the amplitude of accretion rate variation is constant throughout the evolution while the maximum and minimum accretion rates decrease exponentially with the e-folding timescale $t_{\rm evol}$ as defined in § 2. In the model calculations, the maximum accretion rate does not exceed the Eddington accretion rate, $\dot{m} = 1$, and the variability is taken to be periodic in cosmic time. Owing to the redshift dependence of timescale, the variability in the redshift unit depends on the redshift epoch. The duty cycle, the ratio of the elapsed time of QSO in the active phase and the quiescent phase, $t_{\rm act}/t_q$, essentially characterizes the outburst timescale in the disk instability model. There are two important simplifying assumptions that we adopt here in order to make the calculations possible. First, an identical set of period and amplitude of variabilities is applied to QSOs regardless of the overall QSO evolution timescale. Second, because the number of parameters required in a relatively simple DSES model is already excessive, the interdependence among these parameters is ignored for practical calculational purposes.

3.1. *Single-Population Model with Disk Instability*

Figure 6 shows the parameter dependence of the soft X-ray LFs for DSES model. The thermal instability in the accretion disk occurs continuously over the cosmological timescale. See the QSO light curve for a BH mass of $10^8\ M$ in Figure 6*a*. The amplitude of accretion rate variation, $\Delta \log \dot{m}$ is set at 1 and the accretion rate changes without much gain in mass. Because the BH gains most of its mass during an early active phase, the masses of BHs in this model do not grow substantially. Therefore, it is required that the sample QSOs experiencing thermal-viscous ionization instabilities in accretion disks have more massive seed BHs in order to fit the observed LF and MF. The maximum of accretion rate starts from 1 in Eddington unit at the time of birth, and subsequently it falls exponentially below the critical rate, $\log \dot{m}_c = -2$ causing the transition of accretion flow from thin disk (HS) to ADAF (LS/OS). A QSO evolving with the larger $\Delta \log \dot{m}$ experiences the ADAF phase earlier and longer than one with the smaller amplitude. The ratio of $t_{\rm act}/t_q = 0.25$ and the number of outbursts of 10^3 mean that QSO spends about 20% in the active phase and about 80% in the quiescent phase, and the timescale for a burst in the active phase, $t_{\rm act}$, is of the order of 10^6 yr, respectively.

From the light curve in Figure 6*a*, we see the dominant redshift dependence of timescale, which shows that in the redshift plot the recurrence timescale shortens toward low redshifts. Figure 6*b*1 gives the LFs that fit the observed ones in this DSES model. In Figures 4*a*3 and 4*a*4, the LFs in various energy bands for DSES and DNES models are displayed. In these disk instability models of a single QSO population, the number density of bright QSOs does not remain constant and it decreases just as in the SEM and NEM models. This is simply because the dim QSOs in quiescent phase effectively disappear in number counting. *Except for this feature*, based on the comparisons between SES and DSES models and between NES and DNES models, we see that there are little differences between them in the overall shape of LFs, which in part implies that the adopted disk instability model (see the best-fit parameters in Table 1) may not be sophisticated enough to catch some potential subtle differences.

From Figure 6*b*1 versus Figure 6*b*4 and Figure 6*b*2 versus Figure 6*b*3, we see the effects of the amplitude of accretion rate variation on the LFs in DSES model. The amplitude at the level of $\Delta \log \dot{m} = 4$ allows the QSO accretion disk to undergo recurrent spectral changes between the HS and the LS/OS. Starting from its birth, a QSO with a time-varying accretion disk spends most ($\sim 80\%$) of its evolution in the quiescent phase. The quiescent phase is comprised of LS and OS as the mass accretion rate fluctuates. A large number of QSOs remain in the very dim luminosity state while dramatically increasing the undetected low-luminosity galactic nuclei. This increase in the number density, which is normalized to match the comoving number density of Miyaji et al. (2000), depends on the amplitude of the mass accretion rate fluctuations. For instance, the derived comoving number density of QSOs (both observed and dormant) in the case of $\Delta \log \dot{m} = 4$ is roughly 10 times higher than that in the case of $\Delta \log \dot{m} = 1$. From Figure 6*b*1 versus Figure 6*b*2 and Figure 6*b*3 versus Figure 6*b4*, we show the dependence of the LF on the duty cycle in the DSES model, and from Figure 6*b*1 versus Figure 6*b*5, the dependence on the burst frequency. The number of bursts 10^4 means that $t_{\rm act}$ for a burst is of the order of 10^5 yr. As the duty cycle shortens, the time elapsed in the quiescent phase of QSO increases and therefore more QSOs tend to stay in the low-luminosity part of LF at any given epoch. The resulting LFs in the panels, however, show that the number of bursts and the duration of the duty cycle do not affect the evolving shape of the LF significantly in contrast to the effects of the amplitude of accretion rate variation.

3.2. *The Multiple Population Model with Disk Instability*

In Figure 4*b*3 and 4*b*4 show the best-fit LFs in various energy bands for DSEM and DNEM models. MFs of remnant BHs corresponding to these LFs appear in Figure 5. Among the multiple population models, there is little difference in the evolving shape of LFs. It is remarkable that even the evolving shape of LF of the DSEM model with $\Delta \log \dot{m} = 4$ is not conspicuously different from those of the

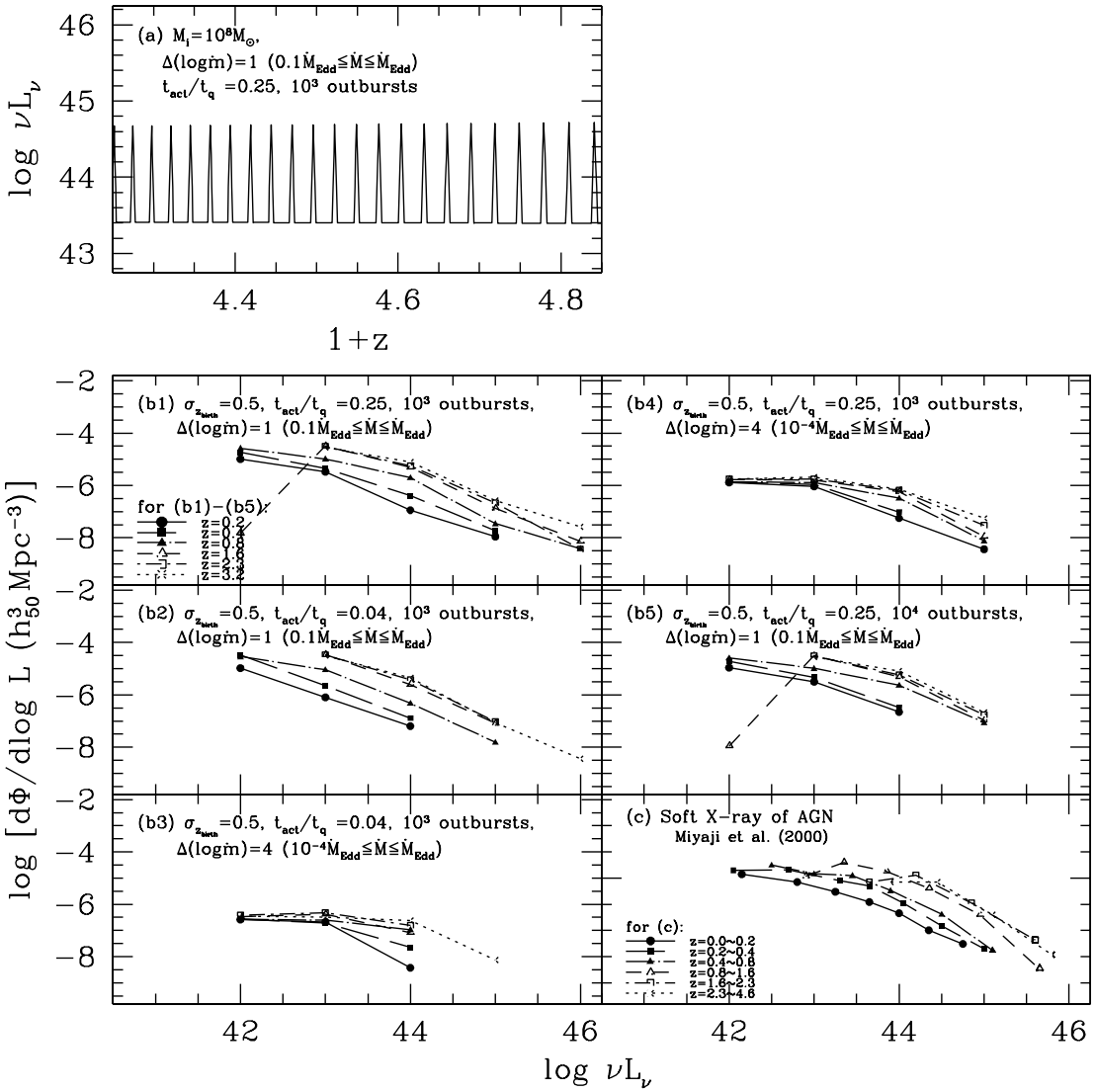

FIG. 6.— (*a*) The light curve of a QSO with an initial BH mass $10^8\,M_\odot$ in the disk instability induced evolution model. (*b1*)–(*b5*) The dependence of the soft X-ray LF on several parameters in a model with a single long-lived QSO population. The QSO population undergoes the long-term luminosity fluctuations and spectral evolution (i.e., DSES model) with the main parameters being the duty cycle between the active and quiescent phases, t_{act}/t_q, the amplitude of accretion rate variation, $\Delta\log\dot{m}$, and the number of bursts. (*b1*) The best fit in this model. The comoving number density is normalized to match that of Miyaji et al. (2000) in (*c*).

other multiple population models. This example demonstrates that the observed LF alone cannot rule out a large number of dormant and hence undetected QSOs/AGNs at any given epoch. This is interesting because the derived comoving number density for this very large amplitude case is substantially bigger (by a factor ~ 10) than those of the other models. This large comoving number density value, however, is still short of the required level in the MF. These results may point to a possibility that within the accuracy of the current models, it is plausible that the QSO accretion disks may indeed undergo the thermal instability and that the observed LFs may well be accounted for by the disk instability model. However, this model has an intrinsic weak point in that it is not directly testable in individual QSOs because the variability timescales expected for AGNs/QSOs in our model are simply too long (e.g., $10^5 \sim 10^6$ yr) and is not directly observable. We also conclude here that the disk instability model cannot simultaneously account for the two observational constraints well enough.

4. DISCUSSION

We have explored diverse types of possible phenomenological scenarios for the cosmological evolution of QSOs. Based on the basic paradigm in which QSOs/AGNs are powered by accreting supermassive black holes (Frank et al. 1992), we have considered various spectral states correlated with the luminosity level (Choi et al. 1999b) and constructed the analytical LFs in the various energy bands. Using the MF of remnant BHs in nearby galactic nuclei as an additional constraint, we have examined whether there exists a model simultaneously satisfying both LF and MF. The best and hence most promising scenario along with the best-fit parameters points to the following formation and accretion history for supermassive BHs and QSOs.

1. In the multiple population models, because of the rapid decrease of $\dot{M}$ caused by the short evolutionary timescale and to the redshift dependence of the evolutionary timescale, the number density of bright QSOs has to evolve strongly over the cosmological time. According to the

derived soft X-ray LFs in a good agreement with observed LFs (Miyaji et al. 2000), the QSOs with less massive seed BHs must have been born more abundantly and/or refueled more efficiently at lower redshifts.

2. While the space number density obtained from the soft X-ray LF of AGNs by Miyaji et al. (2000) is about only 3 times higher than that observed by Boyle et al. (1991), the resulting comoving space densities in the BH remnants inferred from the derived best-fit soft X-ray LFs in all QSO evolution models, which we have tested, are smaller than those estimated for the putative BHs in nearby galaxies by a factor of about 100. This value is larger by a factor of about 10 than those estimated by several authors. No models we have explored can derive the LF and MF satisfying both of the two observational constraints well enough. This could imply that it is highly unlikely that all galaxies contain MDOs that are actually supermassive BH remnants of QSOs. Alternatively, there could be a population of highly obscured AGNs that harbors growing BHs (Fabian 1999; Hasinger 2000).

3. There is little difference in evolving shapes of soft X-ray LFs among all the models we considered. This is inevitable given the fact that our models have at least been required to fit the observed LFs of QSOs/AGNs in the soft X-ray bands (Miyaji et al. 2000). We, however, find substantial differences in optical (4400 Å) LFs and hard X-ray LFs, which is a natural consequence of the assumed spectrum-luminosity correlation (Choi et al. 1999a, 1999b, 2000). In the case of the spectral evolution, the optical LF evolves more rapidly than the X-ray LF, especially at lower redshifts or when QSOs become faint. There is a great difference among the evolving features of the hard X-ray LFs in various models. This is one of the strongest outcomes in the spectral evolution models. Expected observational data by hard X-ray missions such as the *Chandra* X-ray observatory could play a role in providing a much needed, additional observational constraint. Such a constraint will shed light on which QSO models are more plausible and provide a statistical test on whether QSOs have experienced the spectral transition over the cosmological timescale. Such a transition is obviously untestable in individual galaxies owing to the prohibitively long evolution and transition timescales.

4. Two kinds of multiple population model with no spectral evolution (NEM and DNEM models) give the evolving shape of LFs which fit the observed *B* band LF of QSO derived by Boyle et al. (1991) in the optical (4400 Å) band as well. When LF alone is considered, these are quite plausible models among the various evolution models we have tested by far. This result supports the possibility that the QSO population is composed of many short-lived (a few 10^8 yr) generations while in each short generation QSOs do not experience any significant spectral evolution and might undergo the thermal instability in their accretion disks.

This work was supported by a KRF grant 1999-001-D00365. J. Y. was also supported by the MOST through the National R&D program for women's universities. I. Y. wishes to thank Anna I. Yi and Fojyik Yi for numerous discussions and helpful suggestions and Ethan Vishniac for hospitality while this work was in progress.

REFERENCES

Blair, A. J., Stewart, G. C., Georgantopoulos, I., Boyle, B. J., Griffiths, R. E., Shanks, T., & Almaini, O. 2000, MNRAS, 314, 138
Boyle, B. J., Jones, L. R., Shanks, T., Marano, B., Zitelli, V., & Zamorani, G. 1991, in ASP Conf. Ser. 21, The Space Distribution of Quasars, ed. D. Crampton (San Francisco: ASP), 191
Boyle, B. J., Shanks, T., Croom, S. M., Smith, R. J., Miller, L., Loaring, N., & Heymans, C. 2000, preprint (astro-ph/0005368)
Caditz, D., Petrosian, V., & Wandel, A. 1991, ApJ, 372, L63
Cattaneo, A., Haehnelt, M. G., & Rees, M. 1999, MNRAS, 308, 77
Choi, Y., Yang, J., & Yi, I. 1999a, J. Korean Phys. Soc., 34, L199
———. 1999b, ApJ, 518, L77
———. 2000, Nuovo Cimento B, 115B, 165
Comastri, A., Setti, G., & Zamorani, G. 1995, A&A, 296, 1
Di Matteo, T., Esin, A., Fabian, A. C., & Narayan, R. 1999, MNRAS, 305, L1
Esin, A. A., McClintock, J. E., & Narayan, R. 1997, ApJ, 489, 865
Fabian, A. C. 1999, MNRAS, 308, 39
Fabian, A. C., & Canizares, C. R. 1988, Nature, 333, 829
Fabian, A. C., & Rees, M. J. 1995, MNRAS, 277, L55
Franceschini, A., Hasinger, G., Miyaji, T., & Malquori, D. 1999, MNRAS, 310, L5
Franceschini, A., Vercellon, S., & Fabian, A. C. 1998, MNRAS, 297, 817
Frank, J., King, A. R., & Raine, D. 1992, Accretion Power in Astrophysics (Cambridge: Cambridge Univ. Press)
Fukugita, M., & Turner, E. L. 1996, ApJ, 460, L81
Haehnelt, M. G., Natarajan, P., & Rees, M. J. 1998, MNRAS, 300, 817
Haehnelt, M. G., & Rees, M. J. 1993, MNRAS, 263, 168
Hartwick, F. D. A., & Shade, D. 1990, ARA&A, 28, 437
Haiman, Z., & Hui, L. 2000, preprint (astro-ph/0002190)
Haiman, Z., & Loeb, A. 1998, ApJ, 503, 505
Haiman, Z., Madau, P., & Loeb, A. 1999, ApJ, 514, 535
Haiman, Z., & Menou, K. 2000, ApJ, 531, 42
Hasinger, G. 1998, Astron. Nachr., 319, 37
———. 2000, preprint (astro-ph/0001360)
Hatziminaoglou, E., Waerbeke, L. V., & Mathez, G. 1998, A&A, 335, 797
Kauffman, G., & Haehnelt, M. 2000, MNRAS, 311, 576
Madau, P., Chisellini, G., & Fabian, A. C. 1994, MNRAS, 270, L17
Magorrian, J., et al. 1998, AJ, 115, 2285
Mahadevan, R. 1997, ApJ, 477, 585
Mathez, G. 1976, A&A, 53, 15
Mathez, G., et al. 1996, A&A, 316, 19
Mineshige, S., & Shields, G. A. 1990, ApJ, 351, 47
Miyaji, T., Hasinger, G., & Schmidt, M. 2000, A&A, 353, 25
Monaco, P., Salucci, P., & Danese, L. 2000, MNRAS, 311, 279
Narayan, R., Mahadevan, R., & Quataert, E. 1998, in Theory of Black Hole Accretion Disks, ed. Marek A. Abramowicz, G. Bjornsson, & James E. Pringle (Cambridge: Cambridge Univ. Press), 148
Narayan, R., & Yi, I. 1995, ApJ, 452, 710
Nulsen, P. E. J., & Fabian, A. C. 2000, MNRAS, 311, 346
Peebles, P. J. E. 1993, Principles of Physical Cosmology (Princeton: Princeton Univ. Press)
Peterson, B. M. 1997, An Introduction to Active Galactic Nuclei (Cambridge: Cambridge Univ. Press)
Phinney, E. S. 1999, in IAU Symp. 186, Galaxy Interactions at Low and High Redshift, ed. J. E. Barnes, D. B. Sanders (Dordrecht: Kluwer), 94
Richstone D., et al. 1998, Nature, 395, 14
Rutledge, R. E., et al. 1999, ApJS, 124, 265
Salucci, P., Szuszkiewicz, E., Monaco, P., & Danese, L. 1999, MNRAS, 307, 637 (erratum 311, 448)
Siemiginowska, A., Czerny, B., & Kostyunin, V. 1996, ApJ, 458, 491
Siemiginowska, A., & Elvis, M. 1997, ApJ, 482, L9
Small, T. A., & Blandford, R. D. 1992, MNRAS, 259, 725
Wandel, A. 1999, ApJ, 519, L39
Weedman, D. W. 1986, Quasar Astronomy (Cambridge: Cambridge Univ. Press)
Wisotzki, L. 2000a, A&A, 353, 853
———. 2000b, A&A, 353, 861
Yi, I. 1996, ApJ, 473, 645
Yi, I., & Boughn, S. P. 1998, ApJ, 499, 198
———. 1999, ApJ, 515, 576